Domain structure and switching behavior of anisotropic gels

R. A. M. Hikmet and H. M. J. Boots
Philips Research Laboratories, Professor Holstlaan 4, 5656 AA Eindhoven, The Netherlands
(Received 2 November 1994)

Experimental evidence is given for the existence of two types of optically anisotropic gels prepared from mixtures of liquid-crystalline monomers and nonreactive liquid crystal (LC). In type 1 gels, the polymer network is present as an irregular mesh of fine fibrils within the LC. In type 2 gels the liquid crystal is confined in domains separated by thin polymer walls. The switching properties are characterized by the voltage dependence of the transmission and the birefringence and by the time dependence of the transmission response on an instantaneous voltage switch. A theoretical model is introduced to relate the differences in the switching behavior of the two types of gels to their different morphologies.

PACS number(s): 61.30.Gd, 64.70.Md

I. INTRODUCTION

Over the past decade, cells containing nematic liquid crystal (LC) in a polymer matrix have become a viable alternative for twisted nematic cells in a number of applications. The most studied systems of this kind are polymer-dispersed liquid crystals (PDLCs); for a review, see [1]. In PDLCs, the polymer matrix is optically isotropic with a refractive index matching the ordinary refractive index of the liquid crystal in the dispersed phase. If no voltage is applied, the cell scatters light; if a sufficiently high voltage is applied across the cell, the director in the liquid-crystalline droplets turns parallel to the field and the cell is transparent for perpendicularly incident light. Thus one may switch between a scattering off-state and a transparent on-state. If the light is not perpendicularly incident, however, matching of the pertinent effective refractive index is not achieved and the on-state is not totally transparent.

Anisotropic gels [2–5] differ from PDLCs in that the matrix is optically anisotropic such that all components of the dielectric tensor are the same for the matrix and for the liquid crystal. Anisotropic gels are prepared by mixing nonreactive liquid crystal with LC monomers and by polymerizing the mixture in the liquid-crystalline state. After polymerization, the optical axes of the matrix and the liquid are parallel, so that anisotropic gels are transparent in the off-state, irrespective of the angle of incidence of the light. By applying a voltage that turns only the optical axis of the liquid droplets, an optical contrast is created between matrix and droplets and the system scatters.

The rich switching behavior of PDLCs has been the subject of many thorough experimental and theoretical studies [1,7–13]. Here we present simple analytical and numerical models for the description of the switching behavior of anisotropic gels, and we check them experimentally. These models point to the existence of two regimes: one in which the cell walls dominate the switching, and one in which the domain walls are dominant. Anisotropic gels of both types have been prepared, and their transmission and birefringence have been measured as functions of voltage. Additional experimental information is obtained from the time dependence of the switching process.

II. EXPERIMENT

The structures of the reactive LC molecules 1 and 2 used in this study are shown in Fig. 1. The nonreactive LC TL214 was obtained from Merck Ltd. (Poole). The reactive LC molecules were provided with 1% photoinitiator Irgacure 651 and mixtures containing various amounts of the reactive LC (plus the initiator) in TL214 were produced. These mixtures were placed in cells provided with uniaxially rubbed polyimide (PI) layers and transparent indium tin oxide electrodes. Within the cells the LC mixtures became uniaxially oriented under the

1

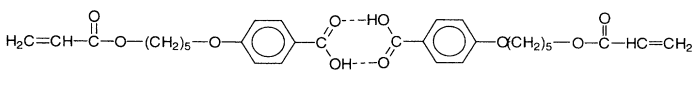

2

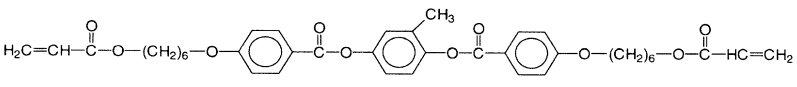

FIG. 1. Molecular structure of the LC acrylates 1 and 2.

1063-651X/95/51(6)/5824(8)/$06.00

influence of the PI layers. Polymerization of monomers 1 and 2 in the mixtures were initiated using a fluorescent light source (1 mW/cm^2) with an emission peak at 360 nm. In this way an anisotropic polymer network was produced containing LC molecules that were not chemically attached to the network. The temperatures of polymerization for monomers 1 and 2 were 25 °C and 50 °C, respectively. Transmission voltage measurements on the gels were carried out using a helium-neon laser and a photodiode at a collection angle of 1°. The frequency of the electric field used for switching was 1 kHz. Birefringence was measured using a calcite compensator and a polarizing microscope. The voltage and the light intensity were registered as a function of time on a digital oscilloscope.

III. MODELS OF ANISOTROPIC GELS

A. An analytical expression for the threshold voltage

In PDLCs the boundary conditions at the droplet-matrix interface are usually such that the director is parallel or perpendicular to the interface. This leads to a variety of director patterns, even for spherical droplets. In the literature threshold voltages have been derived as functions of the Frank elastic constants, the dielectric tensor, the LC-matrix interaction, and the shape of the droplets.

In anisotropic gels, the director at the interface is preferentially parallel to the orientation of the mesogenic units that constitute the polymer network. This orientation is the same throughout the system. As a consequence, the analysis of the threshold behavior for anisotropic gels is much simpler than for PDLCs. Moreover, the droplet shapes may be complicated in anisotropic gels, so that there is a need for a simple model that does not depend critically on the exact droplet shape.

In our study, we consider a cell $0<\alpha<d_\alpha$ with $\alpha=x,y,z$; d_z is the cell thickness and d_x, $d_y \gg d_z$. At the cell walls strong anchoring in the X direction is assumed; the homeotropic case is treated in an analogous way. In order to find an analytical expression for the threshold voltage of anisotropic gels, we model the polymer matrix as a series of N_α planes perpendicular to the three α directions; the distance between the planes is $\delta_\alpha=d_\alpha/(N_\alpha+1)$. This is not a precise model of the microscopic structure of the polymer network, but a tractable idealization of a matrix with many voids. However, as will be seen below, one of the gel types (type 2) has a structure that resembles this model. Similar models involving lines or points instead of planes yield similar results; these models bear more resemblance to type 1 gels. After polymerization in the nematic state, the fixed average optical orientation of the polymer and the director of the liquid crystal will be in the X direction due to the anchoring at the walls. A sufficiently strong electric field in the Z direction will turn the director of the liquid crystal over an angle ϕ in the XZ plane. This rotation is counteracted by the anchoring forces at the wall and by the stiffness of the oriented network. Just above the threshold field the angle ϕ is infinitesimal [14] and the orientational free-energy density is modeled as

$$f(\vec{r})=\tfrac{1}{2}K[\nabla\phi(\vec{r})]^2-\tfrac{1}{2}\epsilon_0\Delta\epsilon E^2[\phi(\vec{r})]^2+P(\vec{r})[\phi(\vec{r})]^2 . \tag{1}$$

For the purposes of this simple qualitative model we only use one Frank elastic constant K. The network influence is modeled by the last term in Eq. (1); it has the effect of locally favoring orientation in the X direction and thus of counteracting the external field. In the analytical model the network is only present in periodic arrays of planes in the X, Y, and Z directions: the parameter $P(\vec{r})$ describing the strength of the network contribution to the orientational free-energy density is taken as

$$P(x,y,z)=P_x\sum_{n=1}^{n=N_x}\delta(x-n\delta_x)+P_y\sum_{n=1}^{n=N_y}\delta(y-n\delta_y)+P_z\sum_{n=1}^{n=N_z}\delta(z-n\delta_z) . \tag{2}$$

In the Appendix it is shown that the threshold voltage $V_{\rm th}$ for this model is given by

$$V_{\rm th}=\pi[(1+m_x+m_y+m_z)K/(\epsilon_0\Delta\epsilon)]^{1/2} \tag{3}$$

with

$$\begin{aligned} m_\alpha &= d_z^2\min[\delta_\alpha^{-2},P_\alpha/(\delta_\alpha K\pi^2)] , \quad \alpha=x,y \\ m_z &= d_z^2\min[\delta_z^{-2}-d_z^{-2} , P_z/(\delta_z K\pi^2)] , \end{aligned} \tag{4}$$

where the minimum of the arguments of min should be taken. We see that the threshold voltage is only independent of the cell thickness if $m_x,m_y,m_z \ll 1$. If one or more of the m_α is not negligible ($\alpha=x,y,z$), but the average matrix influence P_α/δ_α is still small compared to $K\pi^2/\delta_\alpha^2$, the dependence of threshold voltage on the cell thickness will yield not δ_α but an upper bound for δ_α. If a droplet reaches from the top to the bottom of the cell ($m_z=0$) and the width of the largest droplets is roughly three times the cell thickness, Eq. (3) tells us that the threshold voltage is only 10–20 % higher than in the absence of a polymer matrix.

B. Numerical calculations

The analytical model yields an expression for the threshold voltage, but does not predict the optical properties above threshold. Therefore, numerical calculations were performed that yield the birefringence as a function of the voltage for a given distribution of droplet sizes. These calculations are based on Eq. (1), generalized to account for different twist, splay, and bend Frank elastic constants. Since Eq. (4) shows that the threshold voltage depends similarly on the domain sizes in the X, Y, and Z directions, we did not consider domain sizes in the X and Y directions in the numerical model, but restricted ourselves to a simple multilayer model of polymer and LC by taking the network orientation strength P in Eq. (1) as a function of z only. Thus our numerical model is specifically aimed at describing the birefringence; a model for light scattering as a function of voltage should involve

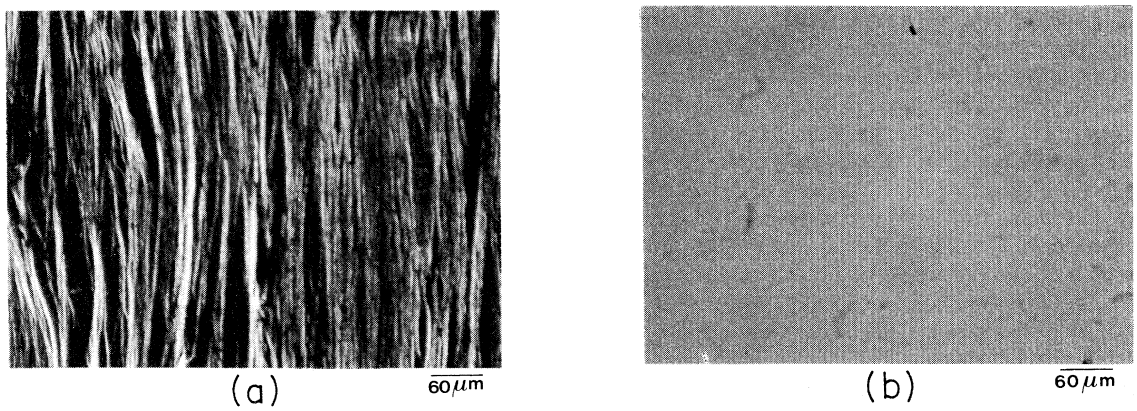

FIG. 2. Optical micrographs of gels of type 1 (left) and 2 (right) obtained between crossed polarizers at a temperature where the LC is in the isotropic phase. The optical orientation of the network is parallel to the cell walls.

x and y dependence of the molecular orientations.

In our model arbitrary functions $P(z)$ may be used. This implies that an arbitrary distribution of domain sizes is possible and that the influence of the network in the polymer-rich regions may be a function of the position z. These points are discussed in Sec. IV.

IV. RESULTS AND DISCUSSION

A. Two types of gels

From the theoretical calculations the possibility of two regimes influencing the switching behavior of the LC molecules in the presence of the anisotropic network is predicted. In one regime the influence of the polymer network on the switching is small, the threshold field is determined by the cell thickness, and the threshold voltage is independent of the cell thickness. In the other regime, the threshold field is determined by the size of the largest domains, and the threshold voltage is proportional to the cell thickness. These regimes and the crossover from one regime to the other are expressed in Eq. (3).

In our previous publications [2–5], various properties of anisotropic gels were discussed. In the production of gels, a mixture of reactive and nonreactive LC molecules is macroscopically aligned and polymerization is photochemically induced. In this way one obtains an anisotropic gel consisting of a polymer network and LC molecules. In our previous publication [5] on gels with homogeneous orientation, infrared dichroism was used to show that the monomeric units of the polymer network and the LC are highly oriented in the same direction. The high orientation of the units of the network is an essential difference between anisotropic gels and systems like PDLC and LC in porous glass, where the network is not oriented.

Here we have chosen two different types of LC acrylate (see Fig. 1), which can lead to two different types of networks. Type 1 and 2 gels were obtained by the polymerization of monomers 1 and 2 at zero applied voltage in the presence of nonreactive TL214 molecules. Both types of gels are as transparent as the unreacted monomer-LC mixtures. Upon application of a voltage across the gels they become increasingly translucent and scatter light. These uniaxially oriented gels preferentially scatter light polarized linearly in the direction of molecular orientation. Further in the text we describe results obtained using this polarization direction.

In Fig. 2 optical micrographs of the gels obtained between crossed polarizers are shown. The photos were obtained after heating the gels above the clearing temperature of the TL214 so that only the polymer molecules would appear birefringent. The photos clearly show the difference in the morphology of the gels obtained using two different monomers. In the type 1 gel, the presence of birefringent polymer fibrils is clear; a sketch of the structure is given in Fig. 3(a). Type 1 gels have also been reported by other authors [6]. The structure of type 2 gels is totally different. On the basis of our previous experiments, we proposed a morphology as sketched in Fig. 3(b) [5]. In type 2 gels the LC is confined in domains separated by thin walls of the anisotropic network. The optical micrograph of the type 2 gel does not show any structure due to the fact that structural variations in the direction perpendicular to the plane of the photograph

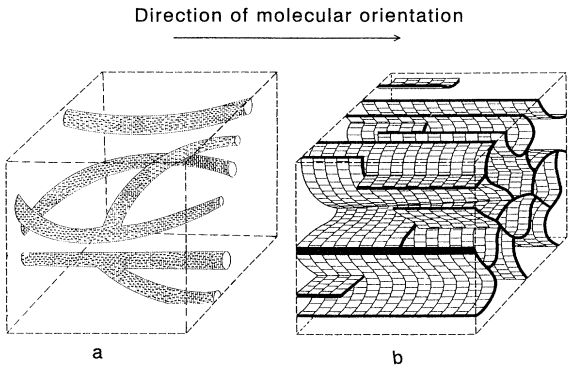

FIG. 3. Sketches of the polymer network structure of type 1 gels [Fig. 3(a)] and of type 2 gels [Fig. 3(b)]. The LC has not been indicated.

are averaged out. The structure in the photograph of the type 1 gel does not allow a direct measurement of the domain size relevant for switching by a voltage, since the nematic-isotropic transition in such a system cannot simply be related to a Fréedericksz transition.

B. Transmission as a function of voltage

In Fig. 4 the transmission voltage behavior of the gels is shown for various polymer concentrations in a 6-μm cell. It can be seen that in the case of the gels of type 1 the threshold voltage (V_{th}) for scattering remains almost constant with increasing network concentration, while the minimum voltage to cause maximum scattering increases slightly. In the case of gels of type 2, both the threshold voltage and the minimum voltage to cause maximum scattering increase rapidly with increasing network concentration. These effects are associated with the size of the domains and their distribution within the network. The fact that the two types of gels show different behavior demonstrates the importance of the polymer structure on the phase behavior within the system.

From Fig. 4 it can be seen that gels of type 1 exhibit a large hysteresis, whereas there is hardly any hysteresis in type 2 gels. This difference can be ascribed to the different morphologies of the two types of gel. Hysteresis occurs when LC molecules follow a route to reorient themselves when the voltage is increased, which is different from the route followed when the voltage is decreased. In the case of conventional display cells, orientation layers ensure uniaxial orientation of the molecules. The hysteresis-free operation of the cells is due to the fact that the LC molecules that are strongly anchored to the orientation layers "guide" the LC molecules in the bulk. A similar situation occurs in type 2 gels, where the anisotropic network layers parallel to the cell walls force the LC molecules in a uniaxial orientation. Polymer layers separate different layers of LC, so that each LC layer may be viewed as a very thin cell with strong uniaxial anchoring at the boundaries. In type 1 gels, the LC phase is continuous. If a voltage is applied to a type 1 gel, the presence of fibrils promotes the formation of domains where the director is oriented in different directions intermediate to the anchoring and the field direction. These domains are not bounded by polymer at all sides, so that many configurations are possible that have almost the same energy, but different domain boundaries. In this view the hysteresis is caused by the frustration of the director in the LC at domain boundaries when the voltage is decreased.

Now we will show that in the present experiments, the two gel types represent two regimes of the threshold behavior modeled in the preceding section. In Fig. 5, the transmission-voltage curves for the two gel types are plotted for various cell gaps. In this figure it can be seen that for the type 1 gels V_{th} shows almost no dependence on the cell thickness, indicating that the domain size within these gels is large compared to the cell thicknesses used.

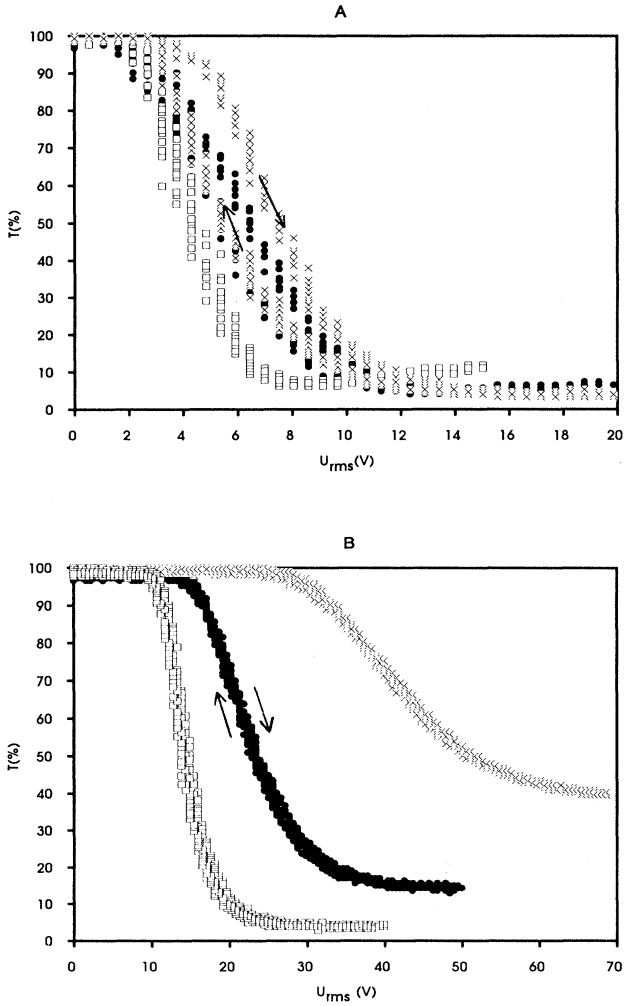

FIG. 4. Transmission-voltage plots of gels of type 1 [Fig. 4(a)] and 2 [Fig. 4(b)] at different concentrations of polymer in a 6-μm cell. Squares, filled circles, and crosses indicate polymer volume fractions of 5%, 7.5%, and 10%, respectively.

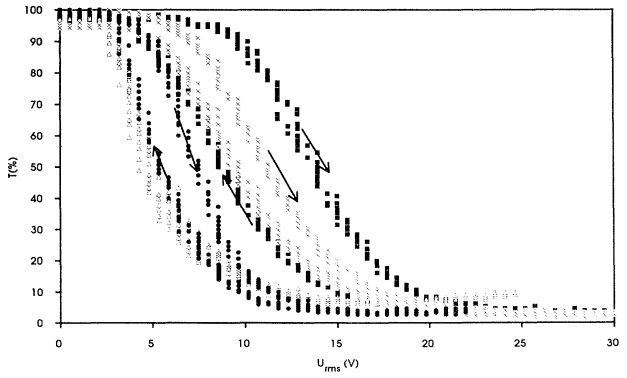

FIG. 5. Transmission-voltage plots of type 1 gels for different values of the cell thickness at a polymer volume fraction of 5%. Curves applying for increasing and for decreasing voltages are indicated by arrows. Triangles, circles, crosses, and squares indicate results for cell thicknesses of 6, 9, 14, and 18 μm, respectively.

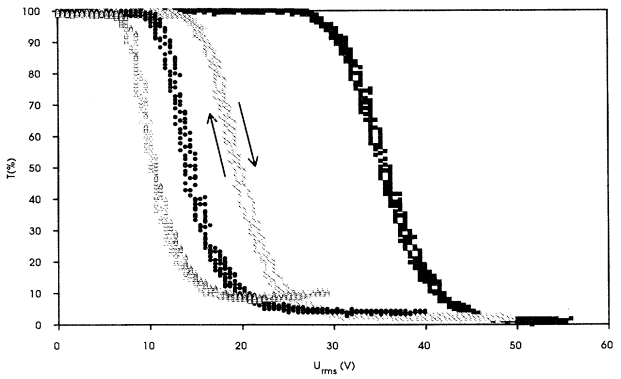

FIG. 6. Transmission-voltage plots of type 2 gels for different values of the cell thickness. The meaning of the symbols is the same as in Fig. 5.

According to the model, this corresponds to the case $m_x, m_y, m_z \ll 1$, which may be realized either by a small orienting influence of the network, or by domain dimensions $\delta_x, \delta_y \gg d_z$ and $\delta_z \approx d_z$.

For the type 2 gels, a strong thickness dependence is observed. In Fig. 6 it can clearly be seen that $V_{\rm th}$ and the minimum voltage for maximum scattering increase with increasing cell thickness d_z. Equation (3) predicts a linear relationship between $V_{\rm th}^2$ and d_z^2; this relation is checked in Fig. 7 for type 2 gels of two polymer concentrations. It can be seen that for both concentrations a linear relationship was obtained in accordance with the model. The extrapolated value at $d_z=0$ must yield the threshold voltage for the pure LC. In the present case it is 2 V and may be neglected. According to the theory, the slopes of the lines are related to the interaction parameters P_α and characteristic dimensions δ_α defining the domains with the lowest threshold voltage. In order to reduce the number of unknowns, we refer to the morphology sketched in Fig. 3(b) and assume that $\delta_x=\infty$, $\delta_y=\delta_z\equiv\delta$, and $P_x=P_y=P_z\equiv P$. Then Eq. (3) may be simplified to

$$V_{\rm th}=\pi d_z[2mK/(\epsilon_0\Delta\epsilon)]^{1/2}\ , \tag{5}$$

with

$$m=\min[\delta^{-2},P/(\delta K\pi^2)]\ .$$

As the parameter P is not known, the model only allows the calculation of an upper limit for the domain size. We deduced from Fig. 7 that $\delta(5\%)\leq 1.4$ μm, and $\delta(10\%)\leq 0.7$ μm. Because of our simplifying assumptions these values are to be considered as order-of-magnitude estimates only. Note that the sizes determined in this way are the sizes of the domains that determine the threshold; these will be the larger domains in the domain size distribution.

C. Switching times

Figures 8 and 9 show the switching speeds of the two different types of gels in cells of various thicknesses. In all cases we tried to obtain roughly the same switching-on time $t_{\rm on}$ for various cell gaps by adjusting the applied voltage. The switching-off time ($t_{\rm off}$), on the other hand, was measured after removing the applied voltage and short-circuiting the cell and did not depend on the applied voltage. The figures show a pronounced dependence of $t_{\rm off}$ on cell thickness for type 1 gels and no cell thickness dependence for type 2 gels. Apart from numeric factors that describe the specific geometries, the switching times are given as [8,14]

$$t_{\rm on}^{-1}=\epsilon_0\Delta\epsilon E^2/\gamma_1-t_{\rm off}^{-1} \tag{6}$$

and

$$t_{\rm off}^{-1}=K/(d_c^2\gamma_1)\ , \tag{7}$$

where γ_1 is the rotational viscosity and d_c is a characteristic length scale for the switching process; depending on the system, d_c may either be the cell gap or a typical domain size. In type 1 gels, the switching-off time does increase with cell thickness, but the increase is slower than the quadratic dependence given in Eq. (7). This

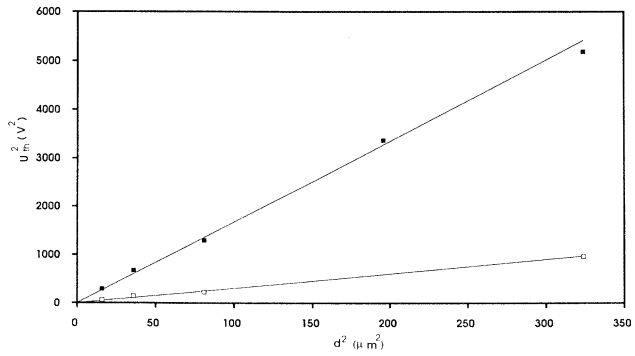

FIG. 7. Squared threshold voltage as a function of squared cell thickness for type 2 gels at two different concentrations of polymer (5% and 10%). The lines are best fits through the data, keeping the threshold voltage at zero thickness equal to the threshold voltage of the pure LC.

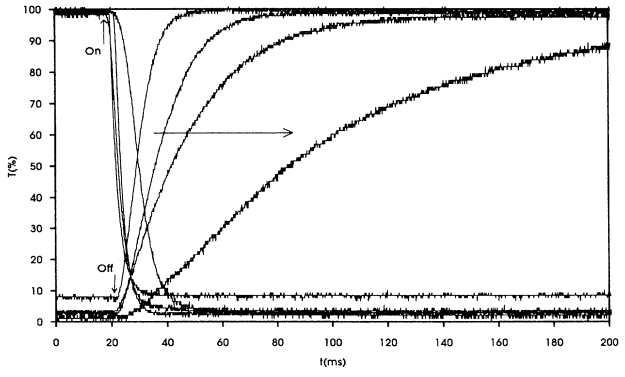

FIG. 8. Transmission-time plot for instantaneous switching in type 1 gels. Decreasing (increasing) curves apply to switching the voltage on (off). The various curves relate to cell thicknesses of 6, 9, 14, and 18 μm. The arrows indicate the order of the curves for increasing cell thickness.

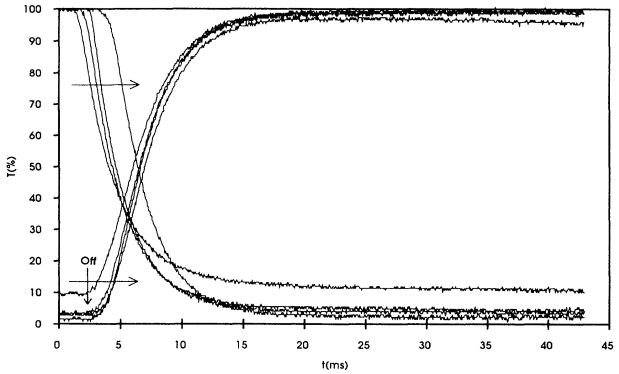

FIG. 9. Transmission-time plot for instantaneous switching in type 2 gels. Symbols and notation are the same as in Fig. 8.

discrepancy need not be due to the presence of the network, since even for pure LC, deviations from the simple Eqs. (6) and (7) are found.

In type 2 gels, switching is determined by the size of the LC domains within the network. This is concluded not only from the dependence of the threshold voltage on the cell thickness, but also from the independence of the switching-off time from the cell thickness. Figure 10 presents the effect of polymer concentration for type 2 gels in 6-μm cells. It can be seen that with increasing polymer concentration t_{off} shows a slight decrease, but this decrease is not as dramatic as the increase observed in the threshold voltage (Fig. 5). This behavior can be explained by considering a distribution of domain sizes within the system. Then d_c is some weighted average over the domain sizes. The weight function in this averaging is determined by the amount of scattering for each domain size. In Fig. 10 it is also clear that the maximum scattering decreases with increasing polymer concentration. This indicates that at higher polymer concentration the domains scatter less effectively, either because the smallest domains in the distribution of domain sizes become smaller than the wavelength of the light in the medium, or because switching of the LC molecules is not possible in the smallest domains.

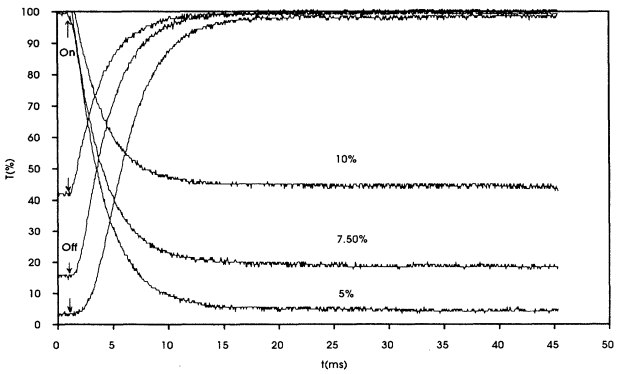

FIG. 10. Transmission-time plot for instantaneous on and off switching of the voltage for type 2 gels in a 6-μm cell. The various curves relate to various polymer concentrations.

D. Birefringence

In order to study the switching of the LC molecules in type 2 gels the effective birefringence as a function of voltage was measured, and the results are shown in Fig. 11. It can be seen that the gels show a V_{th} above which the birefringence decreases almost linearly with increasing voltage. The numerical calculations can be made to approximately match the experimental results at the 10% network if we take 33 vol % of 1-μm LC layers. The calculated birefringence decrease above threshold shows a curvature that is absent in the experiment. Closer matching may easily be obtained by adding thinner LC layers that switch at higher voltages. We used a simple distribution of LC layer thicknesses to illustrate the closer matching (Fig. 11) and the consecutive switching of every smaller domains at increasing voltage (Fig. 12). In a similar way we fitted experimental results at the 5% network. The thickest LC layers are 1 μm and constitute 67 vol % of the cell. We see that the switching behavior is dominated by the largest domains. It is striking that the volume fraction of these domains is much smaller than the volume fraction of LC. Thus a small volume fraction of network has a large influence in constraining the liquid-crystal orientation.

The numerical results of Fig. 11 were obtained by assuming a clear distinction between polymer and LC domains: the LC domains do not contain any polymer, even near the domain boundaries, and in the polymer domains the orienting influence of the network is strong and constant. In the model the polymer segments and the LC molecules are subject to the same LC interaction, but the polymer segments are constrained by the cross-linked polymer network. This constraint is modeled by the third term in the free-energy expression Eq. (1). It has the effect of favoring local orientation in the X direction, which is the direction of orientation at the moment of polymerization. One may think of this term as the free-energy contribution from an effective local field in

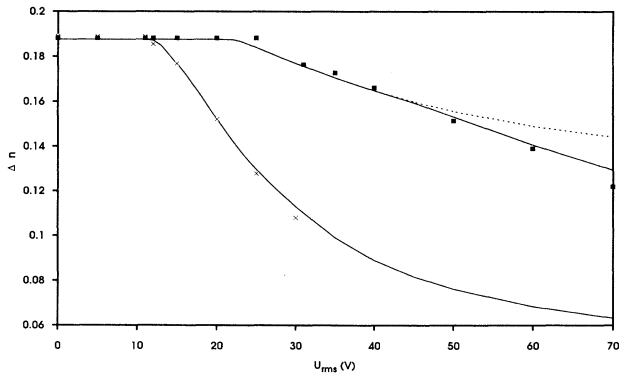

FIG. 11. Birefringence-voltage plot for gels of type 2 in a 6-μm cell. Squares and crosses indicate experimental data for polymer volume fractions of 0.10 and 0.05, respectively. The dotted line is the calculated result for a cell containing 67% of 0.5-μm LC layers. Solid lines are calculated from distributions of layer thicknesses chosen to obtain reasonable fits to the experimental data.

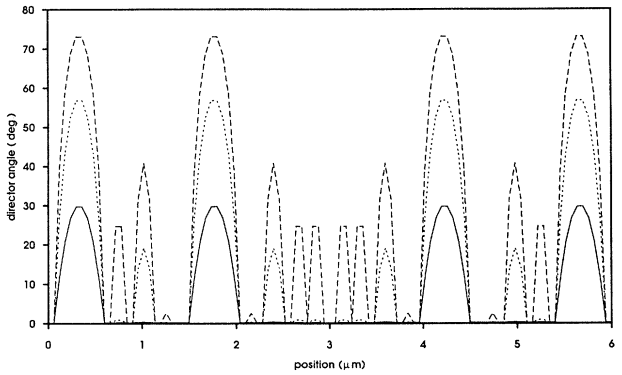

FIG. 12. Director angle as a function of position (Z) in a 6-μm cell calculated by the numerical model. The distribution of LC layer thicknesses is chosen to obtain a reasonable fit to the experimental data at a polymer volume fraction of 0.10. Solid, dotted, and dashed lines are calculated for voltages of 50, 60, and 70 V, respectively.

the polymer domains. When a voltage is applied, there is a competition between this effective local field in the X direction and the external field in the Z direction. Only for loosely cross-linked networks of low stiffness may one assume that the effective local field is not strong and that an external field is able to reorient polymer network segments. However, the network is not perfect and contains an appreciable amount of molecularly dissolved LC molecules that are not chemically, but physically bound to the network. Especially near the boundary between polymer-rich and LC-rich regions, one might expect that the effective local field is weak and continuously varying with position. We have tested the possibilities of weaker networks and of gradual transition regions between different domains by using functions $P(z)$ that have smaller maximum values or finite gradients. [Note that $P(z)$ determines the size and space dependence of the local-field term in the free-energy expression Eq. (1).] Large maximum values and finite gradients resulted in curves similar to the ones shown in Fig. 11, with effective domain sizes. Thus, the experimental results do not exclude transition regions between polymer domains and LC domains. On reducing the maximum value of P as a function of z, however, we found that the clear thresholds in the birefringence-voltage plots became less sharp. Therefore the clear thresholds found in the experimentally determined dependences of the birefringence and the transmission on the voltage support the assumption of a strong fixation of the director orientation in (at least the core of) the polymer domains. This strong fixation of the orientation in polymer domains is also shown in experiments where the anisotropic gels are heated above the clearing temperature: in that case part of the nonreactive LC molecules remains ordered, as observed by infrared dichroism [5].

V. CONCLUSION

We have shown that the two types of anisotropic gels show clear differences in switching behavior. These differences may be interpreted on the basis of simple models. The network of type 1 gels has a fibrillic structure. The interpretation of the threshold behavior by the analytical model points to large domains or to a small polymer-LC interaction. Type 2 gels are characterized by LC domains separated by thin walls of polymer. From the threshold voltages, we determined the dominant domain size and a lower limit for the polymer-LC interaction. Comparison of experimental and theoretical results on the birefringence shows that domains of a size relevant for the switching behavior near the threshold voltage represent a relatively small volume fraction of the LC.

ACKNOWLEDGMENTS

We thank H. A. van Sprang and J. A. M. M. van Haaren for providing us with a computer code for director profiles of pure liquid crystals that has been adjusted to apply to anisotropic gels.

APPENDIX

In this appendix the threshold field is derived for the model described in the text. First, the trivial case of a spatially averaged matrix influence will be treated as a reference. In this case P is constant, so that we may define an effective field $E_{\rm eff}^2=E^2-2P/\epsilon_0\Delta\epsilon$. The Fréedericksz threshold formula for $E_{\rm eff}$ yields

$$E_{\rm th}=\pi\left[\frac{K}{\epsilon_0\Delta\epsilon}\right]^{1/2}\left[d_z^{-2}+\frac{2P}{K\pi^2}\right]^{1/2}. \tag{A1}$$

In the limiting cases of small and large P, we have either the usual inverse proportionality of the threshold field with the cell thickness, or the independence of $E_{\rm th}$ from d_z.

The derivation of the threshold for the model described in the text closely parallels de Gennes's derivation of the Fréedericksz threshold [14]. The anchoring at the cell walls is introduced in a natural way by expanding ϕ in a Fourier series of sines that vanish at $\alpha=0$ and $\alpha=d_\alpha$, where α runs over x, y, and z. On substituting

$$\phi(x,y,z)=\sum_{\nu_x,\nu_y,\nu_z=1}^{\infty}\phi_{\nu_x,\nu_y,\nu_z}\sin(\pi\nu_x x/d_x)\times\sin(\pi\nu_y y/d_y)\sin(\pi\nu_z z/d_z) \tag{A2}$$

into Eq. (1) and integrating over space, we get the total free energy

$$F=\int_{\mathcal{V}}f(\vec{r})d\vec{r}+\tfrac{1}{8}\mathcal{V}\sum_{\nu_x,\nu_y,\nu_z=1}\phi^2_{\nu_x,\nu_y,\nu_z}\left[-\tfrac{1}{2}\epsilon_0\Delta\epsilon E^2+\tfrac{1}{2}K\left[\frac{\pi\nu_x}{d_x}\right]^2+(P_x/\delta_x)\sum_{n=1}^{N_x}\sin^2\left[\frac{\pi\nu_x n}{N_x+1}\right]+\ldots\right], \tag{A3}$$

where $\cdots$ symbolizes terms in y and z analogous to the ones in x and where $\mathcal{V}$ indicates the cell volume. The summation over n yields the value $\frac{1}{2}N_x$, except for the case where ν_x is a multiple of N_x+1; in this case, it vanishes. In looking for the first mode to yield a negative value of F on increasing the field, we must compare the modes

$$(\nu_x,\nu_y,\nu_z)=(1,1,1),(N_x+1,1,1),(1,N_y+1,1),(1,1,N_z+1),$$
$$(N_x+1,N_y+1,1),(N_x+1,1,N_z+1),(1,N_y+1,N_z+1),(N_x+1,N_y+1,N_z+1)\ . \tag{A4}$$

The result of the comparison is given in Eqs. (3) and (4).

[1] J. W. Doane, A. Golemme, J. L. West, J. B. Whitehead, and B.-G. Wu, Mol. Cryst. Liq. Cryst. **165**, 511 (1988).

[2] R.A. M. Hikmet, J. Appl. Phys. **68**, 406 (1990); Liq. Cryst. **9**, 405 (1991); Mol. Cryst. Liq. Cryst. **213**, 117 (1992).

[3] R. A. M. Hikmet and B. H. Zwerver, Liq. Cryst. **10**, 835 (1991); **12**, 319 (1992).

[4] R. A. M. Hikmet and C. de Witz, J. Appl. Phys. **70**, 1265 (1991).

[5] R.A. M. Hikmet and R. Howard, Phys. Rev. E **48**, 2752 (1993).

[6] A. Jákli, D. R. Kim, L. C. Chien, and A. Saupe, J. Appl. Phys. **72**, 3161 (1992); A. Jákli, L. Bata, K. Fodor-Csorba, L. Rosta, and L. Noirez, Liq. Cryst. **17**, 227 (1994).

[7] A. Golemme, S. Žumer, D. W. Allender, and J. W. Doane, Phys. Rev. Lett. **61**, 2937 (1988).

[8] B.-G. Wu, J. H. Erdmann, and J. W. Doane, Liq. Cryst. **5**, 1453 (1989).

[9] J. H. Erdmann, S. Žumer, and J. W. Doane, Phys. Rev. Lett. **64**, 1907 (1990).

[10] R. Ondris-Crawford, E. P. Boyko, B. G. Wagner, J. H. Erdmann, S. Žumer, and J. W. Doane, J. Appl. Phys. **69**, 6380 (1991).

[11] J. Dolinšek, O. Jarh, M. Vilfan, S. Žumer, R. Blinc, J. W. Doane, and G. Crawford, J. Chem. Phys. **95**, 2154 (1991).

[12] S. Kralj, S. Žumer, and D. Allender, Phys. Rev. A **43**, 2943 (1991); S. Kralj and S. Žumer, *ibid.* **45**, 2461 (1992).

[13] S. Žumer, S. Kralj, and J. Bezič, Mol. Cryst. Liq. Cryst. **212**, 163 (1992); S. Žumer and S. Kralj, *ibid.* **12**, 613 (1992).

[14] P. G. de Gennes, *The Physics of Liquid Crystals* (Clarendon, Oxford, 1974).

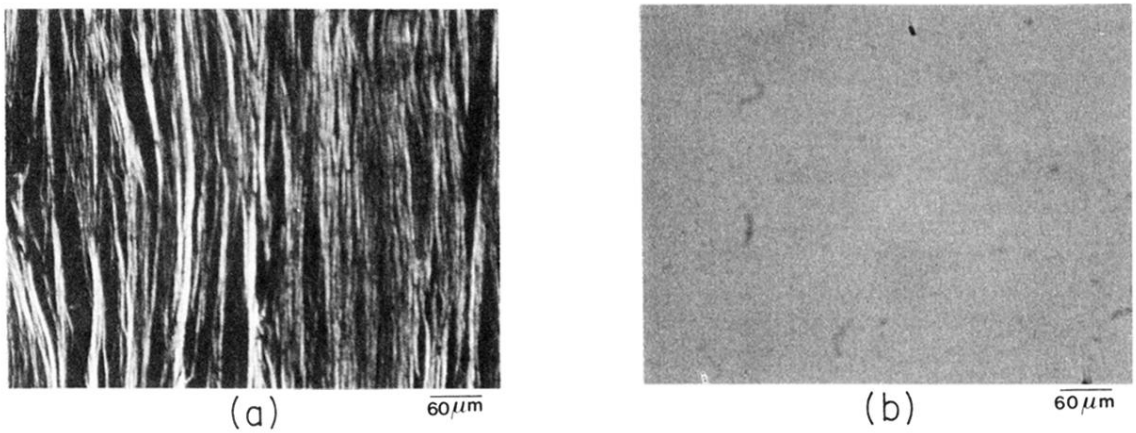

FIG. 2. Optical micrographs of gels of type 1 (left) and 2 (right) obtained between crossed polarizers at a temperature where the LC is in the isotropic phase. The optical orientation of the network is parallel to the cell walls.